IL NUOVO CIMENTO Vol. 36 C, N. 6 Novembre-Dicembre 2013
DOI 10.1393/ncc/i2014-11622-9

Colloquia: LaThuile13

QCD and hadronic physics with KLOE and KLOE-2

S. Miscetti for the KLOE-2 Collaboration
INFN, Laboratori Nazionali di Frascati - via Enrico Fermi 40, Frascati (RM), Italy

ricevuto il 20 Giugno 2013; approvato l'1 Luglio 2013

Summary. — The most recent measurements related to low energy QCD and hadronic physics with the KLOE experiment are reported. We describe the plans for improving the measurement of the Dalitz plot for the $\eta \to 3\pi$ decays which could translate in a better light quark mass determination. We then discuss the measurement of the branching ratio of the $\eta' \to \pi^+\pi^-\gamma$ decays and of its mass spectrum. The high statistical samples collected in the ϕ Dalitz decays to η and π^0 are also presented highlighting the precise determination of the Form Factor slopes and the implication in the search for the U, a hypotethical light vector gauge boson mediating dark forces. Finally we show the first KLOE results for $\gamma\gamma$ physics focusing on the η samples and on the determination of the width $\Gamma(\eta \to \gamma\gamma)$. Perspectives for selected analysis items in the KLOE-2 experiment are also reported.

PACS 13.40.Gp – Electromagnetic form factors.
PACS 14.40.Be – Light mesons ($S = C = B = 0$).
PACS 14.70.Pw – Other gauge bosons.

1. – The KLOE and KLOE-2 experiments

The KLOE experiment operated at DAΦNE, the e^+e^- Frascati ϕ-factory. From 2000 to 2006, KLOE collected $2.5\,\mathrm{fb}^{-1}$ of collisions at the ϕ meson peak and about $240\,\mathrm{pb}^{-1}$ below the ϕ resonance ($\sqrt{s} = 1\,\mathrm{GeV}$). The ϕ meson predominantly decays into charged and neutral kaons, thus allowing KLOE to make precision studies in the fields of flavor physics, low energy QCD and test of discrete symmetries [1]. Properties of pseudoscalar and scalar mesons have been extensively studied using high statistic samples of these particles produced through ϕ radiative decays and $\gamma\gamma$ interactions. The KLOE detector consists of a large cylindrical drift chamber, DC, providing precise momentum resolution, surrounded by a lead-scintillating fiber electromagnetic calorimeter, EMC, that covers almost fully the solid angle and add to a reasonable energy resolution excellent timing performances. A superconducting coil provides a 0.52 T magnetic axial field.

In 2008 the LNF Accelerator Division tested a new interaction scheme, for DAΦNE, which allowed to reduce the beam size and increase of a factor of three the peak luminosity [2]. Following the success of this test, a new data-taking campaign of the

KLOE experiment with an upgraded detector (KLOE-2) has been proposed and a detailed description of its physics program can be found in ref. [3]. The KLOE-2 detector has been successfully installed in this new interaction region and has been initally upgraded only with two small angle tagging devices to detect low (LET) and high (HET) energy electrons or positrons in $e^+e^- \to e^+e^-X$ events ($\gamma\gamma$ physics). The LET, Low Energy Tagger, is made of two LYSO crystal calorimeters, readout by SiPM, placed close to the interaction point. The HET, High Energy Tagger, consists of two scintillator hodoscopes readout by PMT, symmetrically placed after the first bending dipoles of DAΦNE. The DAΦNE commissioning started in 2010, but severe hardware failures lead to a long shutdown period for the machine. The commissioning has been resumed at the end of 2011. In December 2012, the planned shutdown for the installation of the new detectors in KLOE-2 has begun: an inner tracker (IT) and two small angle calorimeters (CCALT,QCALT) to be installed in May 2013. The IT is composed by 4 layers of triple GEM detectors with very light support positioned in close proximity to the interaction point with a UV readout. Its goal is to improve by a factor of 3 the vertex resolution of the central tracker adding four measured points to the extrapolated tracks. The detector has now been completed and is under test. The calorimeters consist of: i) two LYSO crystal calorimeters, CCALT, readout by SiPM, positioned just in front of the innermost quadrupoles to improve the detection of low energy photons at small angle and ii) a heterogeneous calorimeter of reduced thickness ($\sim 5\mathrm{X}_0$), QCALT, composed by 5 layers of W/Cu plates with scintillating tiles readout by WLS fibers connected to SiPM. The QCALT will be used to tag the photons produced by K_L decaying inside the DC and hitting the quadrupoles. Both calorimeters have been assembled and are being qualified.

In the following, we report the most relevant analysis items based on KLOE data that are related to low energy QCD and light hadronic physics. We expect to start data taking with the KLOE-2 experiment this year and collect, in 3 years of runnning, a statistics of $\mathcal{O}(10)\,\mathrm{fb}^{-1}$. Figure of merits for improvements of selected analysis items will be shown.

2. – $\eta \to 3\pi$ decays and determination of light quark masses

The study of the $\eta \to 3\pi$ allows to access the light quark masses since it proceeds through isospin violating operators and its decay rate is proportional to the d and u quark mass difference. The amplitude of the decay can be parametrized as

$$A(s,t,u) = \frac{M_k^2(M_k^2 - M_\pi^2)}{3\sqrt{3}M_\pi^2 F_\pi^2 Q^2} M(s,t,u), \tag{1}$$

where s, t and u are the Mandelstam variables and Q^2 is defined as the quark mass double ratio $Q^2 = \frac{m_s^2 - \hat{m}^2}{m_d^2 - m_u^2}$, with $\hat{m} = \frac{1}{2}(m_d + m_u)$. By measuring the Dalitz plot density of this decay Q^2 can be determined thus help constraining the light quark masses. With a sample of $450\,\mathrm{pb}^{-1}$, we have constructed the Dalitz plot for the $\eta \to \pi^+\pi^-\pi^0$ and $\eta \to 3\pi^0$ decays. The first sample consisted of $\sim 1.3 \times 10^6$ events and has been fit with a polinomial expansion around the Dalitz plot center as follows:

$$|A(x,y)|^2 = 1 + aX + bY^2 + cX + dX^2 + eXY + fY^3, \tag{2}$$

where $X = \sqrt{3}\frac{E_+ - E_-}{\Delta}$ and $Y = 3\frac{E_0 - m_0}{m_\eta - 2m_\pm - m_0} - 1$ are the two Dalitz independent variables. The fit results (see table I) [4] show that: i) the c and e parameters are compatible

TABLE I. – *Fit parameters of the fit to the Dalitz Plot for* $\eta \to \pi^+\pi^-\pi^0$. *Fit* $P(\chi^2)$ *is* 73%.

a	$-1.090 \pm 0.005^{+0.008}_{-0.019}$	d	$0.057 \pm 0.006^{+0.007}_{-0.016}$
b	$0.124 \pm 0.006 \pm 0.010$	e	$-0.006 \pm 0.007^{+0.005}_{-0.003}$
c	$0.002 \pm 0.003 \pm 0.001$	f	$0.14 \pm 0.01 \pm 0.02$

with zero as expected since they are charge conjugation violating; ii) the quadratic slope in Y does not agree with the Current Algebra prediction $b = a^2/4$; iii) a large cubic term in Y is needed to assure a good description of the data. When repeating the fit by forcing $f = 0$ the $P(\chi^2)$ lowers to $\sim 10^{-6}$. The Dalitz plot of the neutral decay $\eta \to 3\pi^0$ follows a symmetric parametrization around the center such as $|A|^2 \propto 1 + 2\alpha Z$ where $Z = \frac{2}{3}\sum_{i=1}^{3}(\frac{3E_i - m_\eta}{m_\eta - 3m_\pi})^2$. A clean sample of 6.5×10^5 fully neutral events is selected in the same data-set used for the $\eta \to \pi^+\pi^-\pi^0$. From the fit, we get the slope $\alpha = -0.0301 \pm 0.0035^{+0.0022}_{-0.0036}$ in good agreement with previous measurements [5].

Dispersive approaches to the $\eta \to 3\pi$ amplitudes have been recently proposed by Colangelo *et al.* [6], where the authors fix the subtraction constants by fitting our measurement of $\eta \to \pi^+\pi^-\pi^0$. They obtain a good agreement with the measured shape and are also able to reproduce the negative slope of the neutral decay. They derive $Q = 21.3 \pm 0.6$. Similar approch has been followed also by another group [7] which extract a close value of $Q = 23.1 \pm 0.7$. A new analysis of the charged channel on the full KLOE data-set is in progress to reduce the systematic uncertainties. Example of data and Monte Carlo shapes for the first $500\,\mathrm{pb}^{-1}$ analized are shown in fig. 1. The decay $\eta' \to \pi^+\pi^-\pi^0$ can be also related to $m_d - m_u$; at present only the measurement by CLEO exists, based on 24 events. At KLOE-2 with $5\,\mathrm{fb}^{-1}$ we expect to collect about 8000 of such events.

3. – The $\eta \to \pi^+\pi^-\gamma$ decay

The decay $\eta \to \pi^+\pi^-\gamma$ proceeds through the box anomaly, a term of higher order with respect to the triangle anomaly. Previous measurements date back to the 70's. The analysis of those two data-sets show some contradictions, in particular concerning the need of a Contact Term (CT) beside the resonant one, dominated by a ρ exchange,

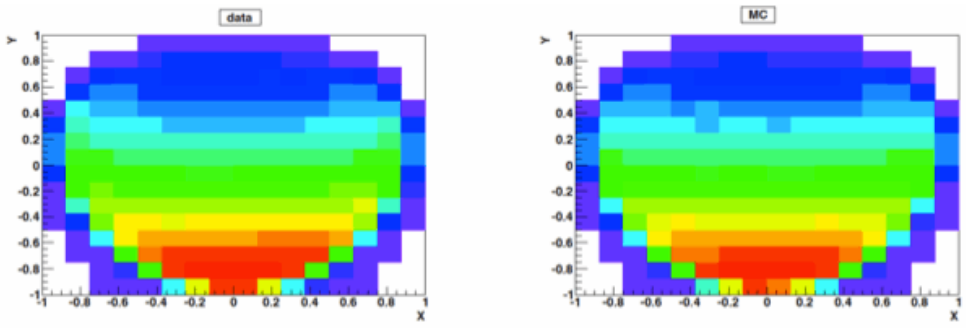

Fig. 1. – $\eta \to \pi^+\pi^-\pi^0$ Dalitz plot density for $500\,\mathrm{pb}^{-1}$ of e^+e^- collisions. Left: data, right: Monte Carlo samples.

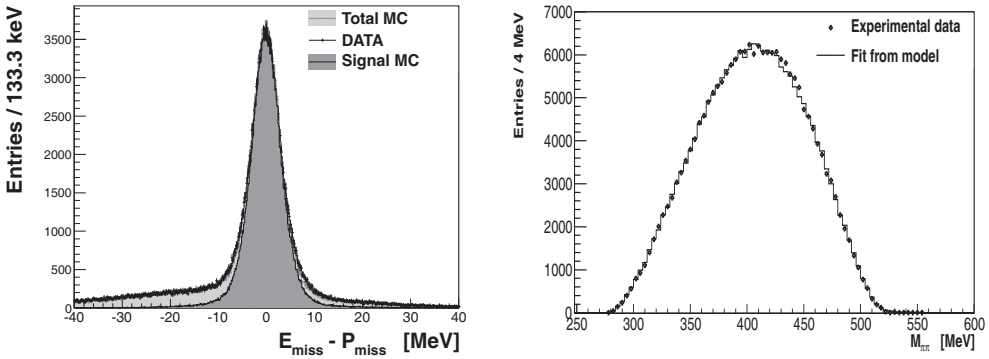

Fig. 2. – Left: $E-p$ distribution for the photon in the $\eta \to \pi^+\pi^-\gamma$ decay. The signal appear as the peak at zero. Right: dipion invariant mass distribution after background subtraction. The histogram is the fit result.

to account for the box anomaly. According to the Hidden Local Symmetry model [8], the value of the partial decay width is sensitive to the CT. Moreover there is a 2–3σ discrepancy between the old BR measurement results $(0.209 \pm 0.004, 0.201 \pm 0.006)$ and the CLEO one [9], 0.175 ± 0.007. From a sample of about $560\,\mathrm{pb}^{-1}$, we extracted 2×10^5 signal events (fig. 2, left).

We found $\frac{\Gamma(\eta \to \pi^+\pi^-\gamma)}{\Gamma(\eta \to \pi^+\pi^-\pi^0)} = 0.1838 \pm 0.0005 \pm 0.0030$ [10], improving by a factor of two the BR precision with negligible statistical error. This result agrees with CLEO and favours a sizeable contribution of the CT [8]. We fitted the $M_{\pi^+\pi^-}$ distribution (fig. 2, right) according to the parametrization of ref. [11], in which the decay width is factorized in a universal non-perturbative part (the pion form factor) and a process specific one $P(s_{\pi\pi}) = 1 + \alpha s_{\pi\pi} + \mathcal{O}(s_{\pi\pi}^2)$ where $s_{\pi\pi} = M_{\pi\pi}^2$. We obtained $\alpha = (1.32 \pm 0.08 \pm 0.10)\,\mathrm{GeV}^{-2}$ in agreement with WASA experiment at COSY [12].

In the case of $\eta' \to \pi^+\pi^-\gamma$ also the $\pi\pi$ invariant mass distribution is expected to be sensitive to the CT [8]. The experimental data are contradictory: in 1997 Crystal Barrel claimed the evidence of the CT while in 1998 the L3 data were well described in terms of resonant contribution only. Therefore a high statistics measurement is desireable. At KLOE-2, with $5\,\mathrm{fb}^{-1}$, $\sim 10^5$ $\eta' \to \pi^+\pi^-\gamma$ events are expected.

4. – Form Factor determination and U boson searches in ϕ Dalitz decays

The Dalitz decay of the ϕ meson, $\phi \to \eta\,\ell^+\ell^-$, have been studied by the SND and CMD-2 experiments, which measured a branching fraction of $(1.19 \pm 0.19 \pm 0.07) \times 10^{-4}$ and $(1.14 \pm 0.10 \pm 0.06) \times 10^{-4}$, respectively corresponding to a cross section of $\sigma(\phi \to \eta\,\ell^+\ell^-) \sim 0.7\,\mathrm{nb}$, in the di-lepton mass range $M_{\ell\ell} < 470\,\mathrm{MeV}$. We have searched for this decay by looking for two main η decay channels, the first in $\pi^+\pi^-\pi^0$ and the second in $3\pi^0$ in a sample of $\sim 1.7\,\mathrm{fb}^{-1}$. The data reduction is very similar in the two cases, the latter one presenting smaller background contamination and higher reconstruction efficiency than the one with four charged tracks. We preselect the sample by requiring 4 (2) tracks coming from a cylinder around the IP and 2 (6) photon candidates and loose cuts around the reconstructed η mass. A clear peak due to ϕ Dalitz events is observed in the distribution of the recoil mass to the e^+e^- pair used to select the final sample.

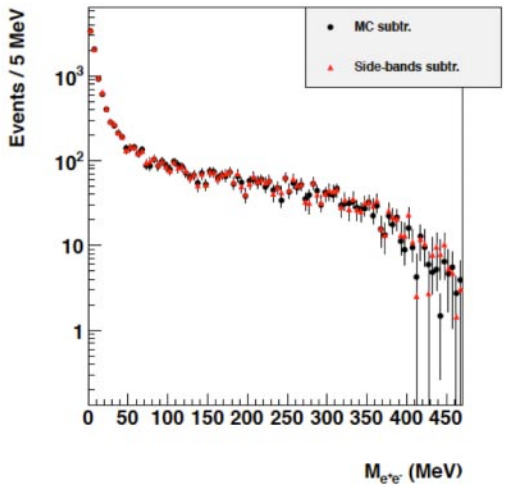

Fig. 3. – Fit to the M_{ee} spectrum for the Dalitz decays $\phi \to \eta\, e^+e^-$, using the $\eta \to \pi^+\pi^-\pi^0$ final state.

Residual background contamination due to photon conversions or other decay chains with charged pions in the final state is suppressed by dedicated algorithms and particle identification methods. A fit is performed to the M_{ee} distribution (see figs. 3, 4) after applying a bin-by-bin subtraction of the residual background. The parametrization of the fitting function has been taken from ref. [13]:

$$(3) \qquad \frac{\mathrm{d}\Gamma(\phi \to \eta\, e^+e^-)}{\mathrm{d}q^2} = \frac{\alpha}{3\pi}\frac{|F_{\phi\eta}(q^2)|^2}{q^2}\sqrt{1-\frac{4m^2}{q^2}}\left(1+\frac{2m^2}{q^2}\right)\lambda^{3/2}(m_\phi^2, m_\eta^2, m_U^2),$$

with $q = M_{ee}$ and the transition form factor,TFF, described by $F_{\phi\eta}(q^2) = 1/(1-q^2/\Lambda^2)$. Free parameters of the fit are Λ and an overall normalization factor. A good description

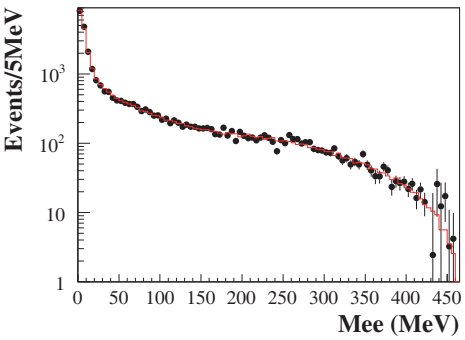

Fig. 4. – Fit to the M_{ee} spectrum for the Dalitz decays $\phi \to \eta\, e^+e^-$, using the $\eta \to \pi^0\pi^0\pi^0$ final state.

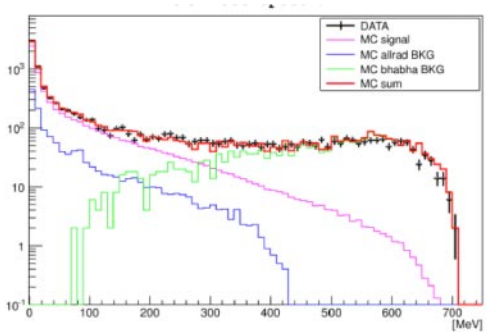

Fig. 5. – Fit to the M_{ee} spectrum for the Dalitz decays $\phi \to \pi^0 e^+e^-$, using the $\pi^0 \to \gamma\gamma$ final state.

of the M_{ee} shape is obtained for both channels. Systematics related to data reduction, analysis corrections and fit ranges is under way. The statistical error achieved for the performed fit is of O(10%) *i.e.* a factor ~ 5 better than obtained by SND ($b_{\phi\eta} = 1/\Lambda^2 = (3.8 \pm 1.8)\,\mathrm{GeV}^{-2}$). A first look at data with respect to MC has also been done for the ϕ Dalitz decay to π^0, with $\pi^0 \to \gamma\gamma$. Observing the Dalitz events in the $e^+e^-\gamma\gamma$ final state is complicated by the presence of a large background coming from Bhabha radiative events. A preliminary data reduction based on cuts of opening angles and invariant masses allows to clean the sample as shown by the M_{ee} distribution reported in fig. 5, where a good signal-over-noise ratio is observed for masses up to $\sim 200\,\mathrm{MeV}$.

The same sample used for the determination of the form factor slopes allows to search for the U boson carrier of the Dark Forces as invoked by theories beyond the Standard Model [14, 15]. Such theories account for a few puzzling astrophysical experimental observations such as, for instance, the excess in the cosmic ray positrons reported by PAMELA, Fermi and, more recently, AMS. These anomalies could all be explained with the existence of a dark matter weakly interacting massive particle, belonging to a secluded gauge sector under which the Standard Model (SM) particles are uncharged. An Abelian gauge field, the U boson with mass near the GeV scale, couples this secluded sector to the SM through its kinetic mixing with the SM hypercharge gauge field. The kinetic mixing parameter, ϵ, is expected to be of the order 10^{-4}–10^{-2} [16,17], so that observable effects can be induced in $\mathcal{O}$(GeV)-energy e^+e^- colliders.

The U boson can be produced at DAΦNE through radiative decays of neutral mesons, such as $\phi \to \eta U$, $U \to l^+l^-$. The expected cross section is expressed by [18]

$$\sigma(\phi \to \eta\, U) = \epsilon^2\, |F_{\phi\eta}(m_U^2)|^2\, \frac{\lambda^{3/2}(m_\phi^2, m_\eta^2, m_U^2)}{\lambda^{3/2}(m_\phi^2, m_\eta^2, 0)}\, \sigma(\phi \to \eta\gamma), \tag{4}$$

where $F_{\phi\eta}(m_U^2)$ is the $\phi\eta\gamma^*$ transition form factor evaluated at the U mass while the following term represents the ratio of the kinematic functions of the involved decays. Using $\epsilon = 10^{-3}$ and $|F_{\phi\eta}(m_U^2)|^2 = 1$, a cross section $\sigma(\phi \to \eta\, U) \sim 40\,\mathrm{fb}$ is obtained. If the U boson exists, it will appear as a sharp peak (2 MeV resolution) over the irreducible background due to ϕ Dalitz decay. The same data used in fig. 3, 4 have been used to extract a limit on the U boson production. This work has been published in [19] and is presented in fig. 6, where the exclusion plot on $\alpha'/\alpha = \epsilon^2$ variable is compared

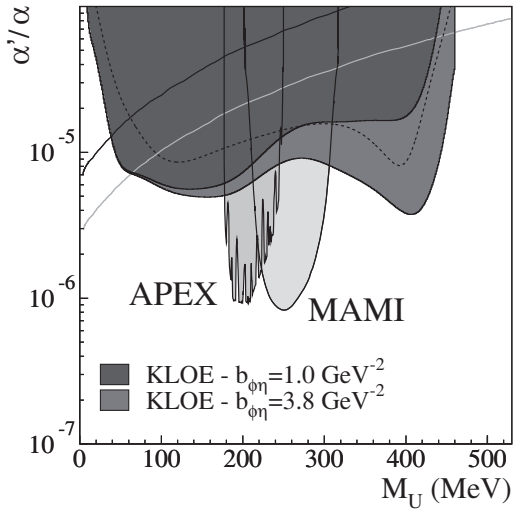

Fig. 6. – Exclusion plot at 90% CL for the parameter $\alpha'/\alpha = \epsilon^2$, compared with existing limits in our region of interest.

with existing limits from the muon anomalous magnetic moment a_μ [20] and from recent measurements of MAMI/A1 [21] and APEX [22] experiments. The evaluation is done in two ways, using the SND experimental value of $b_{\phi\eta}$ or the VMD evaluation ($1\,\mathrm{GeV}^{-2}$). The two resulting curves overlap for low M_{ee} values while the limit based on SND slope gives a better exclusion curves up to 400 MeV. Conservatively, using the VMD slope, we set an upper limit at 90% CL on the α'/α parameter of $\leq 5 \times 10^{-6}$ for $30 < M_U < 190\,\mathrm{MeV}$ and $\leq 1.5 \times 10^{-5}$ for $190 < M_U < 420\,\mathrm{MeV}$.

5. – $\gamma\gamma$ physics: $\eta \to \pi^0\pi^0\pi^0$ and $\eta \to \pi^+\pi^-\pi^0$ final states

In $\gamma\gamma$ processes, $e^+e^- \to e^+e^-\gamma^*\gamma^* \to e^+e^-X$, $C = +1$ hadronic states can be produced. At DAΦNE energies, final states with a single π^0 or η are accessible as well as $\pi\pi$ pairs. In KLOE we can measure these kind of events without the taggers, *i.e.* without detecting the scattered leptons, only by looking at the $250\,\mathrm{pb}^{-1}$ collected at $\sqrt{s} = 1\,\mathrm{GeV}$, where the large background from ϕ decays is largely reduced. In this section, we report the measurement of the two-photon width of the η meson by detecting $e^+e^- \to e^+e^-\eta$ events, with $\eta \to \pi^+\pi^-\pi^0$ and $\pi^0\pi^0\pi^0$.

In figs. 7, 8, the distributions of the missing mass with respect to $\pi^+\pi^-\pi^0$ and $\pi^0\pi^0\pi^0$ are shown. By fitting those histograms we obtain the signal yield and derive the cross sections $\sigma(e^+e^- \to e^+e^-\eta) = (34.5 \pm 2.5 \pm 1.3)\,\mathrm{pb}$ and $\sigma(e^+e^- \to e^+e^-\eta) = (32.0 \pm 1.5 \pm 0.9)\,\mathrm{pb}$ for the charged and neutral η decay channel, respectively. By combining them we evaluate $\sigma(e^+e^- \to e^+e^-\eta) = (32.7 \pm 1.3 \pm 0.7)\,\mathrm{pb}$, from which we extract the most precise measurement to date of the two-photon width: $\Gamma(\eta \to \gamma\gamma) = (520 \pm 20 \pm 13)\,\mathrm{eV}$ [23].

With KLOE-2, we plan to measure $\Gamma(\pi^0 \to \gamma\gamma)$, which is nowadays known with 2.8% accuracy. Running at the ϕ resonance, and by detecting the two scattered leptons in the HET, we can select 10000 $e^+e^- \to e^+e^-\pi^0$ events, with quasi-real photons ($q^2 \simeq 0$), in $5\,\mathrm{fb}^{-1}$ of data, thus allowing us to reach a 1% accuracy in $\Gamma(\pi^0 \to \gamma\gamma)$. We also plan to measure the $\pi^0\gamma^*\gamma$ TFF with a quasi-real photon, $q^2 \simeq 0$, and a virtual one,

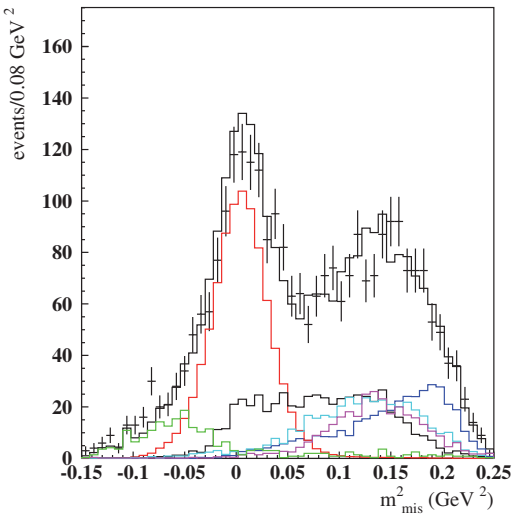

Fig. 7. – Missing mass with respect to $\pi^+\pi^-\pi^0$. Blue: $\gamma\gamma \to \eta \to \pi^+\pi^-\pi^0$, red: $e^+e^- \to \eta\gamma$ with $\eta \to \pi^+\pi^-\pi^0$.

$|q^2| < 0.1\,\mathrm{GeV}^2$, by selecting events in which one of the leptons is detected by the HET and the other one by the KLOE main detector. The available q^2 region is still unexploered and it is important to check the behaviour of the existing TFF parametrizations. Indeed, an accurate measurement of the TFF will reduce the model dependence of the calculation of the Light-by-Light scattering contribution to $(g-2)_\mu$ which is dominated by the single π^0 exchange.

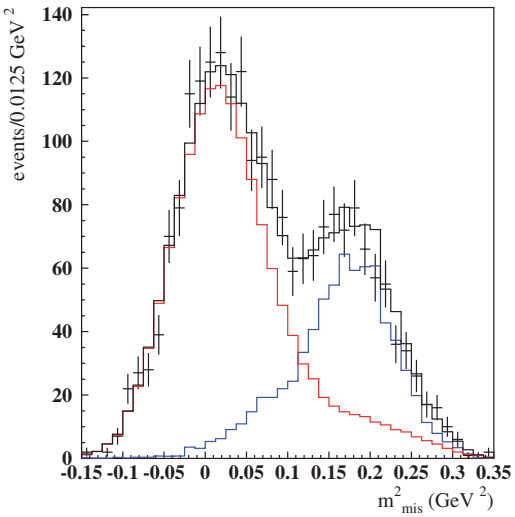

Fig. 8. – Missing mass with respect to the 3 π^0. Blue: $\gamma\gamma \to \eta \to \pi^0\pi^0\pi^0$; red:$e^+e^- \to \eta\gamma$ with $\eta \to \pi^0\pi^0\pi^0$.

6. – Summary and perspectives for KLOE-2

With the upcoming run, we expect to run for 3 runs with the KLOE-2 detector and collect a statistical sample of $\mathcal{O}(10)\,\mathrm{fb}^{-1}$ which will provide an increase of $\times 4$ of available statistics. This, together with the presence of the tagging systems, the improvement on vertex resolution due to the IT, and on the better photon coverage will increase stongly our capability in extracting results in Low energy QCD, kaon physics, quantum-interferometry and γ-γ physics. The feasibility of a high statistics run at 1 GeV, where the resonant background contribution is naturally reduced, is also under discussion.

* * *

This work was supported in part by the EU Integrated Infrastructure Initiative HadronPhysics Project under contract number RII3-CT-2004-506078; by the European Commission under the 7th Framework Programme through the "Research Infrastructures" action of the "Capacities" Programme, Call: FP7-INFRASTRUCTURES-2008-1, Grant Agreement N. 227431; by the Polish Ministery of Science and Higher Education through the Grant No. 0469/B/H03/2009/37.

REFERENCES

[1] Bossi F. *et al.*, *Rivista Nuovo Cimento*, **31** (2008) 531.
[2] Milardi C. *et al.*, *ICFA Beam Dyn. Newslett.*, **48** (2009) 23.
[3] Amelino-Camelia G. *et al.*, *Eur. Phys. J. C.*, **68** (2010) 619.
[4] Ambrosino F. *et al.* (KLOE Collaboration), *JHEP*, **0805** (2008) 006.
[5] Ambrosino F. *et al.* (KLOE Collaboration), *Phys. Lett. B.*, **694** (2010) 16.
[6] Colangelo G. *et al.*, *PoS*, **EPS-HEP2011** (2011) 304.
[7] Kampf K. *et al.*, *Phys. Rev. D.*, **84** (2011) 114015.
[8] Benayoun M. *et al.*, *Eur. Phys. J. C.*, **31** (2003) 525.
[9] Lopez A. *et al.* (CLEO Collaboration), *Phys. Rev. Lett.*, **99** (2007) 122001.
[10] Babusci D. *et al.* (KLOE Collaboration), *Phys. Lett. B.*, **718** (2013) 910.
[11] Stollenwerk *et al.*, *Phys. Lett. B.*, **707** (2012) 184.
[12] Adlarson P. *et al.* (WASA Collaboration), *Phys. Lett. B.*, **707** (2012) 243.
[13] Landsberg L. G., *Phys. Rep.*, **128** (1985) 301.
[14] Fayet P., *Phys. Lett. B.*, **95** (1980) 285.
[15] Batell B., Pospelov M. and Ritz A., *Phys. Rev. D.*, **80** (2009) 095024.
[16] Arkani-Hamed N., Finkbeiner D. P., Slatyer T. R. and Weiner N., *Phys. Rev. D.*, **79** (2009) 015014.
[17] Essig R., Schuster P. and Toro N., *Phys. Rev. D.*, **80** (2009) 015003.
[18] Reece M. and Wang L. T., *JHEP*, **07** (2009) 051.
[19] Babusci D. *et al.* (KLOE Collaboration), *Phys. Lett. B.*, **720** (2013) 111.
[20] Pospelov M., *Phys. Rev. D.*, **80** (2009) 095002.
[21] Merkel H. *et al.*, *Phys. Rev. Lett.*, **106** (2011) 251802.
[22] Abrahamyan S. *et al.*, *Phys. Rev. Lett.*, **107** (2011) 191804.
[23] Babusci D. *et al.* (KLOE-2 Collaboration), *JHEP*, **1301** (2013) 119.